On the Multi-q Characteristics of Magnetic Ground States of Honeycomb Cobalt Oxides

Yuchen Gu[1], Xianghong Jin[1], and Yuan Li[1,2*]

[1]*International Center for Quantum Materials, School of Physics, Peking University, Beijing 100871, China*
[2]*Beijing National Laboratory for Condensed Matter Physics, Institute of Physics, Chinese Academy of Sciences, Beijing 100190, China*

(Received 12 December 2024; accepted manuscript online 24 January 2025)

The Kitaev honeycomb model has received significant attention due to its exactly solvable quantum spin liquid ground states and fractionalized excitations. Layered cobalt oxides have been considered as a promising platform for realizing this model. However, in contrast to the conventional wisdom regarding the single-$\boldsymbol{q}$ zigzag magnetic order inferred from previous studies of the candidate materials Na_2IrO_3 and α-$RuCl_3$, recent experiments on two representative honeycomb cobalt oxides, hexagonal $Na_2Co_2TeO_6$ and monoclinic $Na_3Co_2SbO_6$, have uncovered evidence for more complex multi-$\boldsymbol{q}$ zigzag order variants. This review surveys the experimental strategies used to distinguish between single- and multi-$\boldsymbol{q}$ orders, along with the crystallographic symmetries of cobalt oxides, in comparison with previously studied systems. The general formation mechanism of multi-$\boldsymbol{q}$ order is also briefly discussed. The goal is to provide a solid ground for examining the relevance of multi-$\boldsymbol{q}$ order in honeycomb cobalt oxides and discuss its implications for the microscopic model of these intriguing quantum magnets.

DOI: 10.1088/0256-307X/42/2/027303 CSTR: 32039.14.0256-307X.42.2.027303

1. Introduction. A quantum spin liquid (QSL) is a novel phase of matter in an interacting quantum many-body system.[1,2] Originating from the concept of the resonating valence bond,[3] QSLs have garnered widespread interest, partly because of Anderson's suggestion that resonating valence bonds may be the essence of superconducting pairing in cuprates.[4] A QSL phase does not exhibit spontaneous symmetry breaking even at the lowest temperatures, and features long-range entanglement and fractional quantum excitations.[5] Low dimensionality, magnetic frustration, and strong quantum fluctuations are generally believed to facilitate the formation of QSLs.[6] These considerations are incorporated into the Kitaev honeycomb model.[7] The model, which is defined on a two-dimensional honeycomb lattice with spin-1/2 degrees of freedom and frustrated bond-dependent Ising interactions, has exactly solvable QSL ground states and fractionalized excitations.

Jackeli and Khaliullin first proposed a strategy for materializing the Kitaev model in spin-orbit coupled Mott insulators based on selected transition-metal ions.[8] Over the past decade and a half,[9–11] extensive research has been devoted to 5d-electron iridium-based,[12] 4d-electron ruthenium-based,[13] and most recently, 3d-electron cobalt-based compounds.[14–18] However, the candidate compounds almost always develop long-range magnetic order at low temperatures when the role of disorder is minimized;[9,19–21] thus, the presence of non-Kitaev interactions is evident.[12,22–28] Optimistically, when the non-Kitaev terms are sufficiently small and only act as perturbations to the Kitaev model, it would still be possible to suppress long-range order formation through external tuning.[16,29,30] A commonly considered non-Kitaev term is the isotropic Heisenberg interaction between nearest neighbors. In this context, 3d cobalt-based systems are considered favorable because of a cancellation mechanism that suppresses such Heisenberg interactions.[14–16]

Based on the conventional wisdom attained from studying 4d and 5d materials,[31–33] and following the common practice of using a single-$\boldsymbol{q}$ ansatz in the interpretation of diffraction data,[19–21] the magnetic ground state in some cobaltates was once accepted to be the single-$\boldsymbol{q}$ zigzag order.[17,34,35] However, recent investigations of $Na_2Co_2TeO_6$ and $Na_3Co_2SbO_6$ have uncovered evidence for multi-$\boldsymbol{q}$ order, which can be easily mistaken for the zigzag order with a random domain distribution.[36–41]

In this mini-review, we present an overview of topics pertinent to the formation mechanism of multi-$\boldsymbol{q}$ magnetic order in solids, ranging from crystallographic symmetry considerations to microscopic interactions, as well as experimental methods that can directly or indirectly indicate the existence of such an order. It is hoped that this information will provide a foundation for future work to assess the relevance of the multi-$\boldsymbol{q}$ magnetic order on a more equal footing with the single-$\boldsymbol{q}$ order, in candidate Kitaev materials and beyond, to constrain theoretical models with concrete characteristics of the magnetic ground state.

2. Single-q Order Under Lattice Rotational Symmetry. The formation of magnetic order leads to spontaneous symmetry breaking from the paramagnetic phase. Accurate information on crystallographic symmetry is thus crucial for understanding the symmetry of the magnetic

*Corresponding author. Email: yuan.li@iphy.ac.cn
© 2025 Chinese Physical Society and IOP Publishing Ltd. All rights, including for text and data mining, AI training, and similar technologies, are reserved.

ground state. It is particularly important to examine the transformation of the propagation vector of the single-$\boldsymbol{q}$ order under crystallographic symmetry operations to determine whether it may have a multi-$\boldsymbol{q}$ variant. A recent review [42] provided an excellent summary of the crystallographic and magnetic symmetries of the candidate Kitaev materials.

Na_2IrO_3 [12,43] and α–$RuCl_3$ [31] are the most extensively studied candidate Kitaev materials in the 5d and 4d categories, respectively. Na_2IrO_3 has been established to have a monoclinic $C2/m$ structure through X-ray diffraction on single crystals with a low concentration of stacking faults. [44] In the case of α–$RuCl_3$, extensive research has consistently identified its room-temperature structure as monoclinic $C2/m$. [31,45] However, recent studies have revealed a structural phase transition from $C2/m$ to rhombohedral $R\bar{3}$ upon cooling to temperatures below approximately 150 K. [46–49] The completeness of this transition, along with the thermal transport properties in the low-temperature phase, is highly sensitive to stacking faults in the crystals. [47]

The propagation vectors in both Na_2IrO_3 and α–$RuCl_3$ are characterized by the M-point of the pseudo-hexagonal two-dimensional (2D) Brillouin zone of the honeycomb lattice that is passed through by the C_2-symmetric axis $\boldsymbol{b}$, $\boldsymbol{q} = (0, 1, 1/2)$ [33] and $(0, 1, 1/3)$ [31] in the monoclinic notation, respectively (the difference is in the stacking of the ordered moments along the $\boldsymbol{c}$ axis). Because the 2D wave vector $(0, 1)$ is unique and invariant under monoclinic symmetry operations (Fig. 1), the single-$\boldsymbol{q}$ order has no multi-$\boldsymbol{q}$ variant, and its formation does not necessitate any spontaneous breaking of lattice rotational symmetry. However, in the context of α–$RuCl_3$, this understanding relies on the low-temperature crystal structure being monoclinic. If the genuine crystal structure is $R\bar{3}$, [46–49] the formation of the single-$\boldsymbol{q}$ order may have observable consequences related to the broken C_3 rotational symmetry.

The 3d cobaltates can be thought of as high-spin counterparts to the 5d and 4d systems. [14,15,18] The candidate materials $BaCo_2(AsO_4)_2$, [50,53] $Na_2Co_2TeO_6$, [19,54] $Na_2Co_2TeO_6$ (m) (a monoclinic polymorph), [52] and $Na_3Co_2SbO_6$ [21,54] belong to the space groups $R\bar{3}$, $P6_322$, $C2/m$, and $C2/m$, respectively. The magnetic order in $BaCo_2(AsO_4)_2$ is incommensurate, with $\boldsymbol{q} = (0.27, 0, -1.31)$, [51,55] which is distinct from the other candidate materials. Because of the complexity resulting from incommensurability, the single- versus multi-$\boldsymbol{q}$ nature of the order has not been closely examined in the literature. Nevertheless, we note that the high rhombohedral symmetry of the system would, in principle, allow the order to have multi-$\boldsymbol{q}$ variants. The magnetic orders in $Na_2Co_2TeO_6$ and $Na_3Co_2SbO_6$, which are presumed here to be single-$\boldsymbol{q}$, are characterized by commensurate 2D wave vectors at the M-point of the (pseudo)hexagonal Brillouin zone. [19–21] As shown in Fig. 1, the crystal structure of hexagonal $Na_2Co_2TeO_6$ has C_6 symmetry about the $\boldsymbol{c}$ axis, which introduces three symmetry-related orientational domains that are energetically degenerate, all of which break the lattice rotational symmetry. The cases of monoclinic $Na_3Co_2SbO_6$ and $Na_2Co_2TeO_6$ (m) differ. Although they share the same monoclinic structural symmetry as Na_2IrO_3 and α–$RuCl_3$ (at room temperature), the monoclinic C_2 axis does not pass through the pertinent M-point [21,40,56] (Fig. 1). As a result, the single-$\boldsymbol{q}$ order would break all lattice rotational symmetry. The crystallographic space groups and magnetic wave vectors of different compounds are summarized in Table 1.

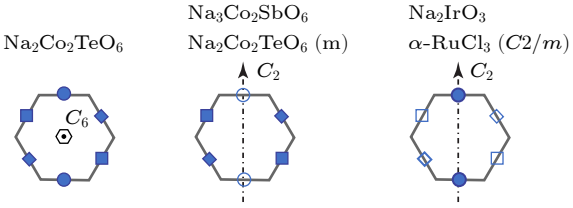

Fig. 1. Magnetic diffraction patterns of different compounds within the first 2D hexagonal Brillouin zone, i.e., without considering the L components. $Na_2Co_2TeO_6$ features three sets of diffraction peaks that are linked by the C_3 rotation. These peaks are produced either together as Fourier components of a triple-$\boldsymbol{q}$ magnetic order, or separately by three types of single-$\boldsymbol{q}$ magnetic domains. Although $Na_2Co_2TeO_6$ (m), $Na_3Co_2SbO_6$, Na_2IrO_3, and α–$RuCl_3$ all possess $C2/m$ space-group symmetry and have a C_2 symmetry axis along $(0, K, 0)$ at room temperature, only $Na_2Co_2TeO_6$ (m) and $Na_3Co_2SbO_6$ have two different sets of symmetry-related magnetic diffraction peaks. Notably, the exact lattice symmetry of α–$RuCl_3$ at low temperatures remains a topic of ongoing discussion.

Table 1. Space groups and magnetic propagation wave vectors of some candidate Kitaev materials. The wave vector of α–$RuCl_3$ employs the monoclinic notation.

–	Space group	Wave vector (r.l.u.)	Refs.
Na_2IrO_3	$C2/m$	$(0, 1, 1/2)$	[33,44]
α–$RuCl_3$	$C2/m$ or $R\bar{3}$	$(0, 1, 1/3)$ $(C2/m)$	[31,47]
$BaCo_2(AsO_4)_2$	$R\bar{3}$	$(0.27, 0, -1.31)$	[50,51]
$Na_2Co_2TeO_6$	$P6_322$	$(1/2, 0, 0)$	[19,20]
$Na_2Co_2TeO_6$ (m)	$C2/m$	$(\pm1/2, 1/2, 0)$	[52]
$Na_3Co_2SbO_6$	$C2/m$	$(\pm1/2, 1/2, 0)$	[21]

As an aside, magnetism in candidate Kitaev materials is traditionally described based on localized magnetic moments on the honeycomb lattice, as they are formed by the atomic spin-orbit coupled $J_{\text{eff}} = \frac{1}{2}$ pseudospins. However, such an ionic picture has been challenged in honeycomb iridium and ruthenium oxides [57–59] based on *ab initio* calculations, which showed that the electronic band width due to inter-site hopping is comparable to the Hubbard repulsion U. It is proposed that an alternative, more accurate low-energy description of the electronic structure involves a linear combination of six t_{2g} atomic orbitals on each hexagon of the honeycomb lattice, called quasi-molecular orbitals (QMOs, in analogy with benzene molecules). Although the precise electronic structure remains a subject of debate, [60–66] it has been argued that the magnetic order in Na_2IrO_3 can also be understood from the QMO perspective. [57] We believe that whether such an order may generally be single- or multi-$\boldsymbol{q}$ (which in turn depends on the lattice symmetry) warrants further investigation, because the electron itinerancy behind QMO formation also promotes higher-order spin interactions in an ionic picture. As discussed in the next section, such higher-order interactions may be intimately linked to

the stabilization of multi-$\boldsymbol{q}$ order.

3. Multi-$\boldsymbol{q}$ Order: Previous Examples. In crystals with sufficiently high rotational symmetry, the conventional single-$\boldsymbol{q}$ magnetic order can break the original rotational symmetry when the symmetry operations do not leave the ordering wave vector invariant. In these cases, a natural method to restore the symmetry is to conceptualize a multi-$\boldsymbol{q}$ variant of the magnetic order, which inherently respects the full rotational symmetry of the material's paramagnetic state. The multi-$\boldsymbol{q}$ magnetic order can be viewed as the vector sum of all symmetry-equivalent single-$\boldsymbol{q}$ components generated by the material's rotational symmetry operations. This summation typically results in a non-collinear or even non-coplanar spin configuration, even when the spins in each individual single-$\boldsymbol{q}$ component are collinear (as long as they are not parallel to the rotational symmetry axis broken by the single-$\boldsymbol{q}$ order). This distinguishing feature sets multi-$\boldsymbol{q}$ magnetic order apart from conventional single-$\boldsymbol{q}$ structures, offering richer and often more complex magnetic textures. Before we discuss multi-$\boldsymbol{q}$ magnetic order in the honeycomb cobaltates, it is useful to survey the formation mechanism and experimental determination of multi-$\boldsymbol{q}$ order in previously studied materials.

In magnetic Hamiltonians with bilinear spin interactions, single- and multi-$\boldsymbol{q}$ magnetic orders are often found to be degenerate in their semiclassical energy.[38,67] Consequently, thermal, quantum, and quenched disorders[67–72] become important factors for selecting the magnetic ground state. A well-known form of multi-$\boldsymbol{q}$ magnetic order is the skyrmion lattice,[73,74] which has been found in a variety of cubic and hexagonal magnetic metals with potential for spintronics applications.[75–77] Skyrmion lattices are believed to be stabilized by the joint effects of thermal fluctuations, external magnetic field, Dzyaloshinskii–Moriya interactions, and magnetization amplitude variations in non-centrosymmetric metallic magnets.[78]

Multi-$\boldsymbol{q}$ magnetic order has also been experimentally observed and theoretically studied in various centrosymmetric systems. Representative materials include cubic[79,80] and tetragonal systems[81–87] (notably, some of the multi-$\boldsymbol{q}$ orders in tetragonal systems are collinear, with spins parallel to the C_4 axis). In these systems, because of the inversion symmetry, Dzyaloshinskii–Moriya interactions are no longer a key driving force, and magnetic frustration and/or spin anisotropy may play important roles.[67,72,88–94] In addition, the effectiveness of long-range (such as dipole-dipole or conduction electron-mediated) and higher-order (such as biquadratic and multi-spin) spin interactions in stabilizing multi-$\boldsymbol{q}$ magnetic order has been highlighted in recent studies.[38,77,80,95–102] Although higher-order interactions in metallic magnets can arise from the interplay between conduction electrons and local moments within a Kondo-lattice picture,[96,103–105] they can also be understood as a natural consequence of the higher-order expansion of the Hubbard model.[106,107] Therefore, the presence of higher-order interactions may be considered as a universal driving force for the formation of multi-$\boldsymbol{q}$ magnetic order in both metallic and insulating systems.

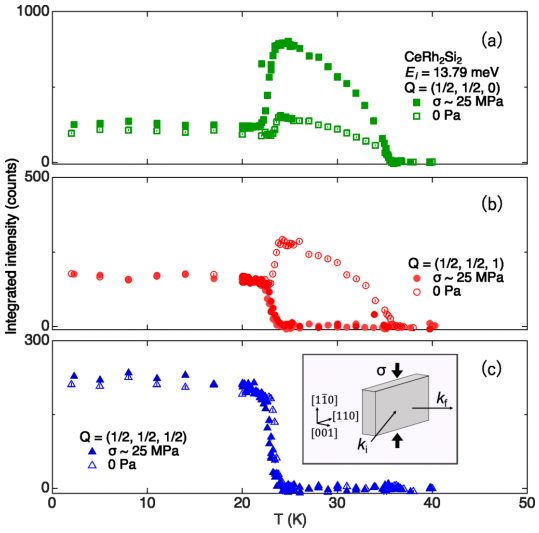

Fig. 2. Temperature dependence of magnetic neutron diffraction intensity in a single crystal of $CeRh_2Si_2$ (inset) cooled with and without uniaxial stress, measured at various wave vectors: (a) $\boldsymbol{Q} = \boldsymbol{q} = (1/2, 1/2, 0)$; (b) $\boldsymbol{Q} = (1/2, 1/2, 1)$, which corresponds to $\boldsymbol{q} = (1/2, -1/2, 0)$ (measured from $\boldsymbol{G} = (0, 1, 1)$, due to the body-centered structure); and (c) $\boldsymbol{Q} = \boldsymbol{q} = (1/2, 1/2, 1/2)$. The first two $\boldsymbol{q}$'s have non-zero intensity in both the single- (between $T_{N1} = 36$ K and $T_{N2} = 25$ K) and multi-$\boldsymbol{q}$ (below T_{N2}) magnetic states, whereas the third $\boldsymbol{q}$ exclusively characterizes the multi-$\boldsymbol{q}$ state. The uniaxial compression σ, applied along the $(1, -1, 0)$ direction, favors the formation of the single-$\boldsymbol{q}$ domain in (a) at the cost of that in (b), but does not strongly affect the multi-$\boldsymbol{q}$ order. This figure is reproduced from Ref. [87] with permission by the American Physical Society.

Distinguishing a rotational symmetry-breaking single-$\boldsymbol{q}$ order from its symmetry-preserving multi-$\boldsymbol{q}$ variant can be challenging in conventional diffraction experiments.[108,109] This is because in both scenarios, the magnetic diffraction intensities at the rotational symmetry-related $\boldsymbol{q}$ vectors are expected to be nearly equal. This equality is intrinsic to multi-$\boldsymbol{q}$ order, but extrinsic in the case of single-$\boldsymbol{q}$ order because of the randomized domain population. A viable strategy to differentiate the two is hence to create an unequal domain population in the latter case by "training" the sample with external symmetry-breaking conditions. An example of this is displayed in Fig. 2, where the magnetic diffraction peaks from a single crystal of $CeRh_2Si_2$ are compared after cooling the sample with and without uniaxial compression.[87] The compression perturbs the symmetry of the Hamiltonian and causes single-$\boldsymbol{q}$ domains to have different formation likelihoods, resulting in variations in the corresponding magnetic diffraction intensities [Figs. 2(a) and 2(b)]. In contrast, the diffraction intensities associated with the symmetry-preserving multi-$\boldsymbol{q}$ order are relatively insensitive to compression [Fig. 2(c)]. Thus, the single- (between 25 K and 36 K) and multi-$\boldsymbol{q}$ (below 25 K) nature of the ordered states can be distinguished. Similar experiments using strain or magnetic fields to "detwin" single-$\boldsymbol{q}$ domains can be found to elucidate the multi-$\boldsymbol{q}$ nature of magnetic order in a variety of materials, i.e., based on the lack of detwinning effects.[77,85,87,110]

It is important to note that even a multi-$\boldsymbol{q}$ order may

break some (but not all) of the rotational symmetry.[109] A notable example is found in cubic $SrFeO_3$,[79] as demonstrated by the measurement data shown in Fig. 3. Similar to the previous example, a magnetic field was applied upon cooling the sample to alter the domain population, as indicated by the intensities of the different magnetic Bragg peaks. The system was in a quadruple-$\boldsymbol{q}$ ordered state in phase II [Figs. 3(a) and 3(c)], as indicated by the absence of clear field-training effects, because the more stable quadruple-$\boldsymbol{q}$ order preserves the full rotational symmetry of the cubic crystal. However, in phase I below 80 K, the more stable magnetic order becomes double-$\boldsymbol{q}$, which allows for the development of orientational domains that are trainable by the field. The training field can be applied either upon the initial cooling [Fig. 3(a)] or at low temperatures after zero-field cooling [Fig. 3(b)], as long as the field is sufficiently large, and the training effect persists even after the field is removed. The training mechanism can be explained as follows. Without an external field, the double-$\boldsymbol{q}$ order naturally develops in 12 randomly distributed domains, each featuring the combinations of two wave vectors among q_1, q_2, q_3, and q_4 (along with time-reversal twins). In a training field, one of the wave vectors (for example, q_1) becomes favored over the other three, such that three of the twelve domains (q_1+q_2, q_1+q_3, and q_1+q_4) are preferred. This causes the double-$\boldsymbol{q}$ order's diffraction intensities at the unfavored wave vectors to remain non-zero and amount to approximately one third of that at the favored wave vector.[79]

Multi-$\boldsymbol{q}$ states can also be identified through specific characteristics that are accessible in diffraction measurements without training the sample. One approach is to search for higher-order harmonic peaks, which can be interpreted as the coherent superposition of distinct $\boldsymbol{q}$ components.[86,111] However, it has been suggested that under certain conditions, specific multi-$\boldsymbol{q}$ states may exhibit zero intensity at the positions of higher-order harmonic peaks.[100] Another approach involves detecting the associated structural symmetry breaking, which reflects magnetoelastic coupling effects in the rotational symmetry-breaking single-$\boldsymbol{q}$ state.[82,83] Although high-resolution X-ray or neutron scattering techniques are required for this purpose because of the typically small induced lattice distortions, symmetry-sensitive probes such as Raman scattering (for observing phonon splitting[112]) may be used as complementary methods.

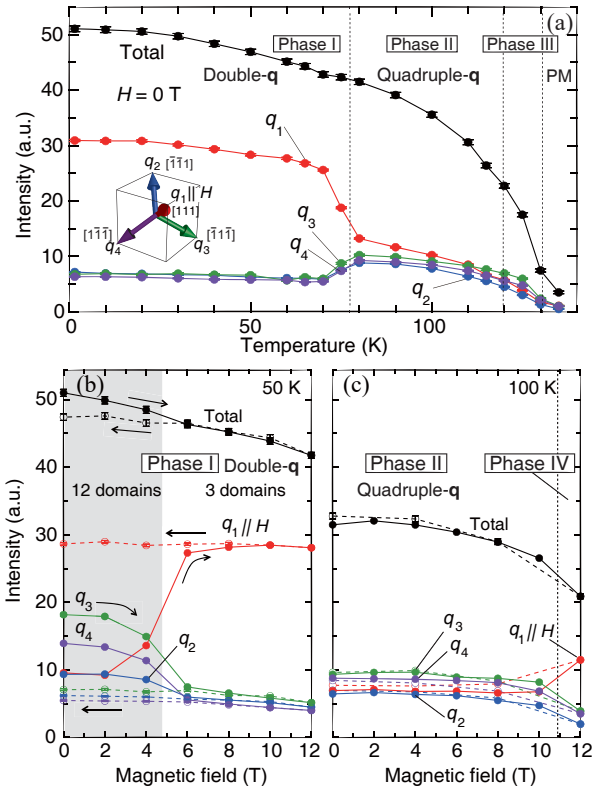

Fig. 3. (a) Temperature dependence of magnetic intensities measured at $\boldsymbol{q}_i$ (i = 1–4) in zero field after field-cooling the sample to the lowest temperature. (b) and (c) Magnetic field dependence of the scattering intensities measured in the double-$\boldsymbol{q}$ phase I and the quadruple-$\boldsymbol{q}$ phase II, respectively. The solid lines and broken lines illustrate data measured upon increasing and decreasing the field along [111], respectively. All the data were measured after zero-field cooling from room temperature. This figure is reproduced from Ref. [79] with permission by the American Physical Society.

Table 2. List of materials with reported multi-$\boldsymbol{q}$ magnetic states, along with the key experimental indications.

–	Crystal structure	Type	Stabilized by	Way to identify	Refs.
Nd	Hexagonal	Metal	N.A.	Higher-order satellites	[111]
Mn-Ni alloy	Face-centered cubic	Metal	N.A.	γ-ray emission	[108]
USb	Face-centered cubic	Metal	N.A.	Excitation spectrum	[113]
$(U_{1-x}Pu_x)Sb$	Face-centered cubic	Metal	N.A.	Field detwinning	[110]
$SrFeO_3$	Simple cubic	Metal	Thermal fluctuations	Field detwinning	[79]
$Y_3Co_8Sn_4$	Honeycomb	Metal	Four-spin interaction	Field detwinning	[77]
$MnTe_2$	Simple cubic	Semiconductor	DM interaction	Mössbauer	[114]
$Co_{1/3}TaS_2$	Triangular	Metal	Four-spin interaction	Excitation spectrum	[115,116]
$Co_{1/3}NbS_2$	Triangular	Metal	Four-spin interaction	Mössbauer	[117]
$CeRh_2Si_2$	Tetragonal	Metal	Biquadratic interaction	Stress detwinning	[87]
$GdRu_2Si_2$	Tetragonal	Metal	Higher-order interaction	Field detwinning	[85]
				Higher-order satellites	[86]
$(Sr_{1-x}Na_x/Ba_{1-x}K_x)Fe_2As_2$	Tetragonal	Superconductor	Biquadratic interaction	Diffraction & Mössbauer	[81–83]
$Ba_2(Y/Lu)RuO_6$	Cubic	Insulator	Biquadratic interaction	Excitation spectrum	[80,97]
$Na_2Co_2TeO_6$	Honeycomb	Insulator	Ring exchange	Excitation spectrum	[36]
				Field detwinning	[39]
$Na_3Co_2SbO_6$	Monoclinic honeycomb	Insulator	N.A.	Field detwinning	[40]

Further signatures of multi-$\boldsymbol{q}$ magnetic states can be found in the local spin orientations. As the electronic magnetic moments can affect the nuclear moments via hyperfine coupling, they can be detected by nuclear technologies such as γ-ray emission[108] and Mössbauer spectroscopy.[81,114,117] Moreover, in some special cases, multi-$\boldsymbol{q}$ states can be recognized using spin-polarized scanning tunneling microscopy[118,119] and nuclear magnetic resonance (NMR).[120] In addition to the static properties, multi-$\boldsymbol{q}$ states can leave signatures in the spin dynamics, which can be measured via inelastic neutron scattering (INS).[80,113,115,116] Evidence for multi-$\boldsymbol{q}$ states may be obtained by either fitting the excitation spectrum[80,113,115] or scrutinizing their characteristic behavior distinct between single- and multi-$\boldsymbol{q}$ states.[116] Table 2 summarizes how multi-$\boldsymbol{q}$ magnetic ground states have been experimentally indicated in various compounds.

4. Evidence for Multi-$\boldsymbol{q}$ Order in Honeycomb Cobalt Oxides As discussed in Section 2 and illustrated in Fig. 1, the crystallographic symmetries of $Na_2Co_2TeO_6$ and $Na_3Co_2SbO_6$ are compatible with M-point magnetic order in either single- or multi-$\boldsymbol{q}$ form. To determine which of these scenarios is more likely to be correct, single-crystal neutron diffraction experiments have recently been performed with in-plane magnetic fields in both $Na_2Co_2TeO_6$[39] and $Na_3Co_2SbO_6$.[40] Here, we focus only on the training effects of the fields on the magnetic domains, as discussed in the previous section.

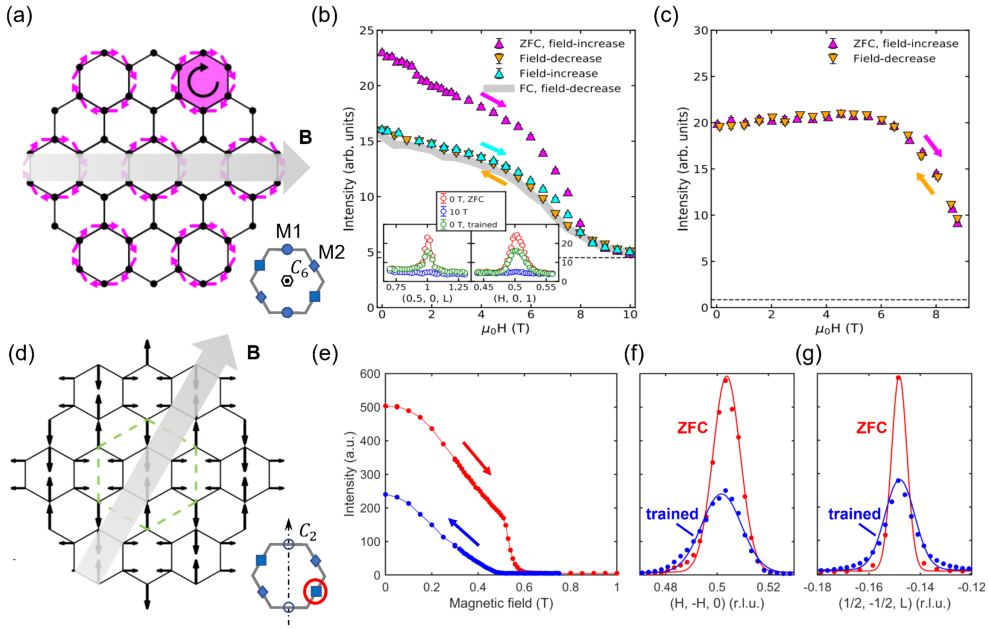

Fig. 4. (a) Schematic of triple-$\boldsymbol{q}$ magnetic structure in $Na_2Co_2TeO_6$, constructed by summing three zigzag components whose propagating wave vectors are different M-points of the Brillouin zone (inset). The direction of the applied magnetic field is unfavorable for the M_1 component. (b) and (c) Field evolution of magnetic Bragg peaks at $M_1 = (0.5, 0, 1)$ and $M_2 = (0, 0.5, 1)$ in $Na_2Co_2TeO_6$ at 2 K. Data displayed in the main panels were measured at the maximum of the peak profile (insets). Horizontal dashed lines indicate background levels. (d) Schematic of double-$\boldsymbol{q}$ magnetic structure in $Na_3Co_2SbO_6$, constructed by summing two zigzag components that are related to each other by the C_2 rotational symmetry about the $\boldsymbol{b}$ axis. With a magnetic field applied along the indicated low-symmetry direction, the zigzag component (circled in the inset) shown in (e)–(g) is expected to be unfavored. (e)–(g) Field evolution and training effect of the magnetic Bragg peak at $(1/2, -1/2, 0)$ in $Na_3Co_2SbO_6$ at 2 K. These figures are adapted from Refs. [39] and [40] with permission by the American Physical Society.

In $Na_2Co_2TeO_6$, the single-$\boldsymbol{q}$ magnetic structure (or single-$\boldsymbol{q}$ component in a multi-$\boldsymbol{q}$ structure) has been constrained[19,20] to have the in-plane component of magnetic moments in each zigzag chain ferromagnetically aligned parallel to the chain, i.e., perpendicular to $\boldsymbol{q}$. The moments are further canted towards the $\boldsymbol{c}$ axis in an alternating fashion between the chains. Assuming that the multi-$\boldsymbol{q}$ variant of the magnetic structure preserves all of the crystallographic rotational symmetries, its in-plane magnetic moment arrangement can be inferred by summing three single-$\boldsymbol{q}$ components 120° from each other,[36,39] which results in an ordering pattern with spin "vortices," as displayed in Fig. 4(a).

In the recent experiments reported in Ref. [39], the magnetic domains in $Na_2Co_2TeO_6$ were trained either at the lowest temperature (2 K) up to a maximal field of 10 T, or upon cooling from the paramagnetic state in a 10 T field, in the field geometry shown in Fig. 4(a). Figures 4(b) and 4(c) present the evolution of magnetic Bragg peak intensities at $M_1 = (0.5, 0, 1)$ and $M_2 = (0, 0.5, 1)$, respectively, demonstrating the effect of training. When the training field was removed, the M_1 intensity recovered to approximately 2/3 of the value originally observed after zero-field cooling, whereas the M_2 intensity returned to its original value without a significant difference. These results show that the training process failed to eliminate the formation of any presumed energetically unfavored single-$\boldsymbol{q}$ domains. Although the 1/3 intensity decrease at M_1 might

indicate partial suppression of the corresponding single-$\boldsymbol{q}$ domain, the lost intensity (measured at integer $L = 1$) was found to be redistributed into rod-like magnetic diffuse scattering along the $\boldsymbol{c}^*$ axis, rather than into diffraction signals at other M points. In other words, although the training affected the magnetic correlation length across the honeycomb layers, there was no indication of a repopulation of single-$\boldsymbol{q}$ orientational domains within the layers.[39] These observations favor a triple-$\boldsymbol{q}$ magnetic ground state in $Na_2Co_2TeO_6$. The only remaining alternative possibility is the existence of unidentified structural pinning effects, such as frozen-in uniaxial strains, which are randomly distributed in the samples yet sufficiently strong to overrule the effects of the magnetic fields. This issue was addressed in a more recent study,[121] in which an emergent effect arising from the spin vorticity [Fig. 4(a)] was observed using optical Faraday rotations.

The experimental situation for $Na_3Co_2SbO_6$ is similar. Here, the question is between single- and double-$\boldsymbol{q}$ scenarios. The double-$\boldsymbol{q}$ magnetic ground state[40] features a non-collinear arrangement of the in-plane magnetic moments [Fig. 4(d)]; however, it has no spin vorticity because of the absence of a third magnetic propagating vector along $\boldsymbol{b}^*$. To differentiate the two scenarios, an in-plane training field was applied in a low-symmetry direction, as illustrated in Fig. 4(d). The measured magnetic Bragg peak [Figs. 4(e)–4(g)] was at the propagating wave vector, which corresponds to domains that are unfavored by the training field in the single-$\boldsymbol{q}$ order scenario. The central finding was that the diffraction signal recovered after the training field was removed, even though the field was sufficiently strong to fully suppress the order. Hence, the recovered signal was more likely a component of the full, double-$\boldsymbol{q}$ order parameter, rather than being associated with a given type of single-$\boldsymbol{q}$ domain. Similar to the case of $Na_2Co_2TeO_6$, the peak intensity decreased after training owing to a broadening of the momentum profile of the diffraction signals [Figs. 4(f)–4(g)], particularly along the $\boldsymbol{c}^*$-axis. After accounting for the broadening, the total intensity was found to be unaffected by the training.[40]

A distinct characteristic of the multi-$\boldsymbol{q}$ ordering patterns shown in Figs. 4(a) and 4(d) is that some sites have smaller ordered moment magnitudes than the rest. In $Na_2Co_2TeO_6$, the sites that have zero in-plane moments are expected to have ordered moments along the $\boldsymbol{c}$-axis, which give rise to the ferrimagnetic behavior of the system[124] in the ordered state, and which can be understood as being related to the spin canting[19,20] in the individual zigzag components. However, the magnitudes of these moments are not expected to be equal to the in-plane ones because the system has a pronounced overall easy-plane response to external fields.[124] In $Na_3Co_2SbO_6$, the zero-field magnetic structure has been fully determined through spin-polarized neutron diffraction,[40] with varying moments at the lattice sites, as shown in Fig. 4(d). The presence of these reduced ordered moments implies the persistence of spin dynamics deep in the ordered state because of magnetic frustration and quantum fluctuations of the systems, as confirmed by recent muon spin relaxation measurements.[125]

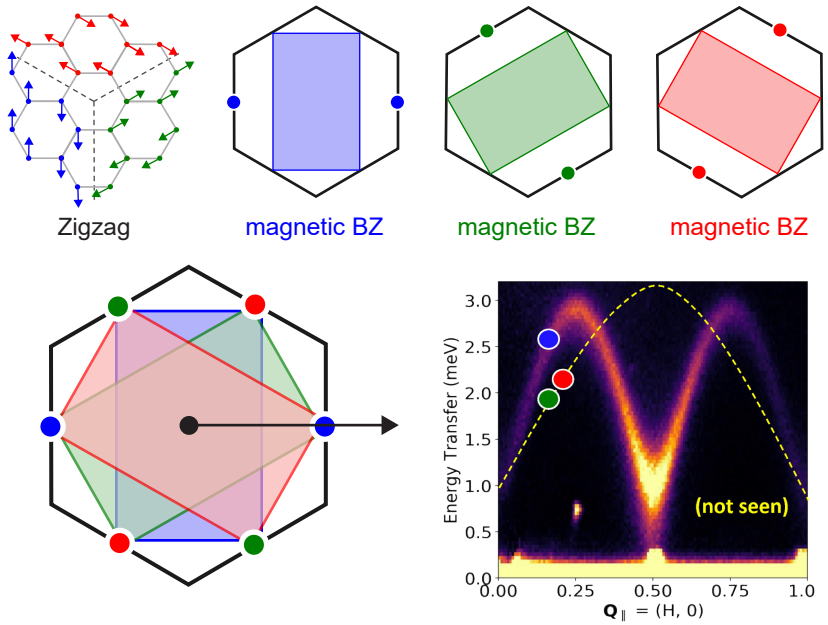

Fig. 5. Upper half: Three orientational domains of the zigzag order, along with their corresponding propagating wave vectors and magnetic Brillouin zones. Lower left: Superposition of three types of magnetic Brillouin zones. When spin waves are measured along the momentum trajectory that connects two neighboring structural Brillouin zones (black arrow), two types of dispersion relations are expected, because the trajectory passes through magnetic zone centers three times in the "blue" domain, but only twice (plus through the zone corner once) in the "green" and "red" domains. Lower right: Experimental spectra are consistent with the understanding that the momentum trajectory passes through magnetic zone centers three times, i.e., without seeing the presumed contributions from the "green" and "red" zigzag domains, hence contradicting the zigzag scenario but being consistent with the triple-$\boldsymbol{q}$ scenario. The figure is adapted and modified from Ref. [36] with permission by the American Physical Society.

The above evidence for multi-$\boldsymbol{q}$ magnetic order in $Na_2Co_2TeO_6$ and $Na_3Co_2SbO_6$ originated from diffraction experiments. Historically, the likelihood of triple-$\boldsymbol{q}$ order in $Na_2Co_2TeO_6$ was first revealed by inelastic neutron scattering experiments based on symmetry arguments.[36] As illustrated in the upper half of Fig. 5, in the zigzag scenario, the three orientational domains feature rectangular magnetic Brillouin zones that are rotated 120° with respect to each other. As a result, in a large, co-aligned sample for inelastic neutron scattering, one expects to observe spin excitations from all three types of domains simultaneously, e.g., with two types of dispersion relations observed in the momentum trajectory displayed in the lower half of Fig. 5. The experimental spectra[36] strongly contradict this expectation, as only one branch of spin-wave dispersion is observed below 3 meV. Instead, the data are fully consistent with a triple-$\boldsymbol{q}$ understanding of the magnetic order, which has a smaller hexagonal magnetic Brillouin zone (corresponding to the overlapping colored region in the lower left panel of Fig. 5).

However, it is important to note that such symmetry arguments alone might not be rigorous, as they cannot be used to rule out zigzag order formation under certain interaction parameter settings. For instance, when the interaction model has only Heisenberg interactions between the third-nearest neighbors (J_3), in which case the zigzag and triple-$\boldsymbol{q}$ orders are degenerate classical ground states, the magnon dispersions of the different zigzag domains are also degenerate. This degeneracy arises because the spin lattice is effectively decoupled into different sublattices, as detailed in a discussion presented in Ref. [126]. However, such degeneracy is not symmetry-enforced, as the absence of interactions between neighbors closer than J_3 is a special requirement. When such interactions are present, fitting the entire INS spectrum[126] (not just the lowest-energy branch) starting from a zigzag ground state, and considering the coexistence of multiple domains, remains a challenge.[34,127,128] Spin-wave fitting based on a triple-$\boldsymbol{q}$ ground state has yielded considerably more satisfactory results,[38] further supporting the triple-$\boldsymbol{q}$ scenario.

In addition to the neutron scattering efforts discussed above, indirect evidence for multi-$\boldsymbol{q}$ magnetic order has been obtained using other experimental techniques. These include null results in Raman scattering detection of phonon energy splitting in $Na_2Co_2TeO_6$,[36] which should be present if the magnetic order (in conjunction with magnetoelastic coupling) strongly breaks the lattice C_6 rotational symmetry about the $\boldsymbol{c}$ axis, as well as nuclear magnetic resonance detection of the local internal fields in both $Na_2Co_2TeO_6$[37] and $Na_3Co_2SbO_6$:[41] a multi-$\boldsymbol{q}$ magnetic ground state is expected to produce more complicated nuclear magnetic resonance spectra than a single-$\boldsymbol{q}$ one.

5. Implications for Theoretical Models. Information on the magnetic ground state imposes strong constraints on microscopic magnetic model construction, providing critical insights into the underlying interactions. As discussed in Section 3, the multi-$\boldsymbol{q}$ order in centrosymmetric itinerant magnets highlights the significant role of long-range and higher-order interactions, which in those cases naturally arise from the interplay between local moments and conduction electrons. In contrast, conventional models for Kitaev-candidate honeycomb cobaltates are based on the tight-binding Hubbard insulator framework; in a first-order approximation, this translates into spin Hamiltonians with only bilinear spin interactions (e.g., Heisenberg and Kitaev interactions between two spins).[14–16,129] Within these models, the semi-classical energies of single- and multi-$\boldsymbol{q}$ orders are usually degenerate;[38,67] however, as displayed in Fig. 6, the ground state can become multi-$\boldsymbol{q}$ order when higher-order spin interactions or magnetic fields are introduced.[122,123,130,131] Indeed, in the case of $Na_2Co_2TeO_6$, a triple-$\boldsymbol{q}$ ground state has been proposed to be stable in the presence of six-spin ring-exchange interactions when the system is near a hidden SU(2)-symmetric point in the parameter space of an extended Heisenberg-Kitaev-Gamma model.[38] Notably, the model provides a satisfactory description of the full experimental spin-wave spectrum.

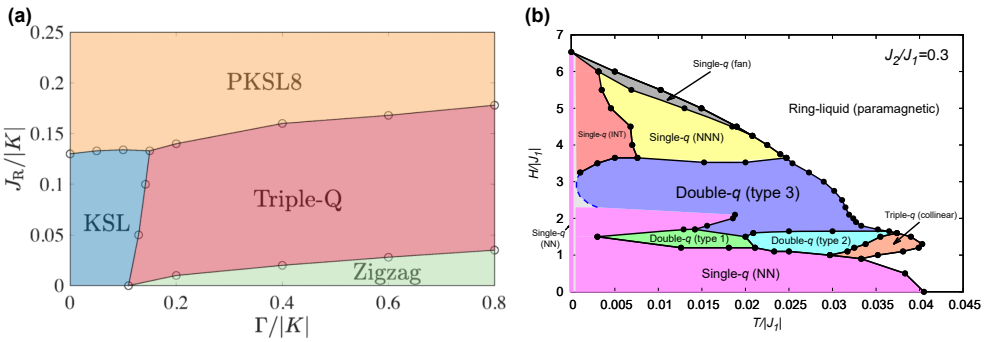

Fig. 6. (a) Phase diagram of the quantum $K-\Gamma-\Gamma'-J_R$ model for $K<0$, $\Gamma>0$, $J_R>0$, and $\Gamma'/|K|=-0.05$ in the limit of large system size, calculated using the variational Monte Carlo method. Two types of QSL phases appear: KSL and PKSL8, near the triple-$\boldsymbol{q}$ phase. (b) The $H-T$ phase diagram of the J_1-J_2 honeycomb-lattice Heisenberg model with $J_2/J_1=0.3$, determined through Monte Carlo simulation. The low-temperature light-gray region is the region where thermalization cannot be achieved, whereas the zero-temperature limit can be identified based on the low-temperature expansion as a single-$\boldsymbol{q}$ (NN) state. The dotted blue line representing the low-temperature phase boundary of the double-$\boldsymbol{q}$ (type 3) state remains somewhat arbitrary. This figure is adapted from Refs. [122] and [123] with permission by the American Physical Society.

Such multi-spin, higher-order interactions are considered to emerge from higher-order expansions of the tight-binding Hubbard model,[38] and their presence underscores the critical role of electron hopping in Mott insulators. The significance of hopping is indicated by the dimensionless quantity t/U, where t and U are the inter-site hopping and on-site repulsion energies, respectively. Traditionally, hopping is expected to be less significant and more short-ranged in cobalt oxides than in extended 5*d*- and 4*d*-electron systems.[14–16] However, a recent detailed analysis of the electronic structure of a candidate material $BaCo_2(AsO_4)_2$,[132] suggested that the hopping energy may have been underestimated. Specifically, the direct xy/xy hopping $t' \sim -300$ meV dominates the superexchange hopping between the xz and yz orbitals via the ligand p states $t \sim 50$ meV. Similar findings have also been reported for $Na_2BaCo(PO_4)_2$ and other edge-sharing Co oxides.[132–134] This contradicts previous assumptions that ligand p state-mediated hopping is predominant in cobaltates[16] as a key factor behind dominant Kitaev interactions. Another significant deviation is the notable hopping between the third-nearest neighbors, which already becomes substantial at the DFT level.[135] According to the inelastic neutron scattering results, the presence of third-nearest-neighbor spin interactions also appears to be a general characteristic of materials such as $BaCo_2(AsO_4)_2$, $Na_2Co_2TeO_6$, and $Na_3Co_2SbO_6$.[34,38,51,126,128]

The validity of microscopic models and their ground states can be further examined via the models' ability to explain related experimental observations. It has been reported for $Na_2Co_2TeO_6$ that, before developing the well-known 3D magnetic order, the system exhibits an intermediate phase featuring an unusual form of 2D order.[36] This phase has recently been explained using a model with ring-exchange interactions.[136] Depending on the sign of the ring-exchange interactions, either a zigzag or a triple-$\boldsymbol{q}$ ground state is favored, and they have intermediate "vestigial" phases in the forms of $\mathbb{Z}_3$ spin-nematic or $\mathbb{Z}_4$ spin-current density wave order, respectively. The experimentally observed vestigial phase in $Na_2Co_2TeO_6$ is consistent with the $\mathbb{Z}_4$ spin-current density wave order.[136] The order breaks lattice translational symmetry but preserves time-reversal symmetry, which explains why it does not lead to pronounced anomalies in magnetic susceptibility or NMR measurements,[19,20,37,124] but can be observed in specific heat and diffraction measurements.[36,39] The same model can explain the experimentally observed ferrimagnetic net moment in the 3D ordered phase as well.[124,137]

6. Summary and Outlook. In summary, we have reviewed how the possible existence of multi-$\boldsymbol{q}$ order in magnetic materials can be experimentally addressed. This can be accomplished using either reciprocal-space methods, such as diffraction under external fields, or real-space methods, such as NMR and STM. Current experimental evidence for such a multi-$\boldsymbol{q}$ magnetic order in the honeycomb cobaltates has followed these routes. The findings extend the relevance of the multi-$\boldsymbol{q}$ type of ordering from itinerant magnets to Mott insulators, promoting a re-examination of previously determined magnetic orders based on a single-$\boldsymbol{q}$ ansatz in similar systems. Because the presence of higher-order and long-range interactions probably plays a crucial role in stabilizing the multi-$\boldsymbol{q}$ order, the results highlight the significance of electron itinerancy even in Mott insulator systems, challenging the conventional theoretical framework that leads to the prediction of dominant Kitaev interactions in the 3*d* honeycomb cobalt oxides.

Despite their likely substantial deviations from the Kitaev honeycomb model, the cobalt oxides retain the potential to host exotic quantum states. As displayed in Fig. 6(a), various spin-liquid phases are predicted to emerge near the triple-$\boldsymbol{q}$ phase.[122] Moreover, in these nearly ideal two-dimensional honeycomb magnets, theoretical studies suggest that a spin-liquid ground state might emerge from competing interactions, particularly between the first and third nearest neighbors.[51,138–141] The observation of a continuum-scattering signal in $BaCo_2(AsO_4)_2$ via THz spectroscopy under a large $\boldsymbol{c}$-axis magnetic field may indicate such a state.[142,143] The inferred unequal-magnitude spin distribution in the multi-$\boldsymbol{q}$ states of $Na_2Co_2TeO_6$ and $Na_3Co_2SbO_6$ suggests that the classical order is suppressed by pronounced quantum fluctuations, a finding corroborated by muon spin relaxation measurements.[125,144] Although these materials finally develop antiferromagnetic order at low temperatures, the tendency of the systems to form ferromagnetic correlations does not fall far behind, and can be enhanced by external fields. Near the critical points between quantum phases featuring these different magnetic correlations, exotic states with enhanced quantum fluctuations may emerge. In parallel with this optimistic view, it is equally important to acknowledge that seemingly novel observations might stem from relatively trivial origins such as disorders and lattice dynamics.[145–149] This highlights the need for careful interpretation of experimental data to distinguish genuine quantum phenomena from extrinsic effects.

Acknowledgements. We are grateful to our coworkers and colleagues for their many fruitful collaborations and stimulating discussions. The work at Peking University was supported by the National Basic Research Program of China (Grant No. 2021YFA1401901) and the National Natural Science Foundation of China (Grant No. 12474138).

References

[1] Broholm C, Cava R J, Kivelson S A, Nocera D G, Norman M R, and Senthil T 2020 *Science* **367** eaay0668
[2] Balents L 2010 *Nature* **464** 199
[3] Anderson P W 1973 *Mater. Res. Bull.* **8** 153
[4] Anderson P W 1987 *science* **235** 1196
[5] Wen J, Yu S L, Li S, Yu W, and Li J X 2019 *npj Quantum Mater.* **4** 12
[6] Zhou Y, Kanoda K, and Ng T K 2017 *Rev. Mod. Phys.* **89** 025003
[7] Kitaev A 2006 *Ann. Phys.* **321** 2
[8] Jackeli G and Khaliullin G 2009 *Phys. Rev. Lett.* **102** 017205

[9] Takagi H, Takayama T, Jackeli G, Khaliullin G, and Nagler S E 2019 *Nat. Rev. Phys.* **1** 264
[10] Motome Y, Sano R, Jang S, Sugita Y, and Kato Y 2020 *J. Phys.: Condens. Matter* **32** 404001
[11] Trebst S and Hickey C 2022 *Phys. Rep.* **950** 1
[12] Chaloupka J, Jackeli G, and Khaliullin G 2010 *Phys. Rev. Lett.* **105** 027204
[13] Plumb K W, Clancy J P, Sandilands L J, Shankar V V, Hu Y F, Burch K S, Kee H Y, and Kim Y J 2014 *Phys. Rev. B* **90** 041112
[14] Liu H and Khaliullin G 2018 *Phys. Rev. B* **97** 014407
[15] Sano R, Kato Y, and Motome Y 2018 *Phys. Rev. B* **97** 014408
[16] Liu H, Chaloupka J, and Khaliullin G 2020 *Phys. Rev. Lett.* **125** 047201
[17] Kim C, Kim H S, and Park J G 2021 *J. Phys.: Condens. Matter* **34** 023001
[18] Liu H 2021 *Int. J. Mod. Phys. B* **35** 2130006
[19] Lefrançois E, Songvilay M, Robert J, Nataf G, Jordan E, Chaix L, Colin C V, Lejay P, Hadj-Azzem A, Ballou R, and Simonet V 2016 *Phys. Rev. B* **94** 214416
[20] Bera A K, Yusuf S M, Kumar A, and Ritter C 2017 *Phys. Rev. B* **95** 094424
[21] Yan J Q, Okamoto S, Wu Y, Zheng Q, Zhou H D, Cao H B, and McGuire M A 2019 *Phys. Rev. Mater.* **3** 074405
[22] Chaloupka J, Jackeli G, and Khaliullin G 2013 *Phys. Rev. Lett.* **110** 097204
[23] Kimchi I and You Y Z 2011 *Phys. Rev. B* **84** 180407
[24] Sizyuk Y, Price C, Wölfle P, and Perkins N B 2014 *Phys. Rev. B* **90** 155126
[25] Rau J G, Lee E K H, and Kee H Y 2014 *Phys. Rev. Lett.* **112** 077204
[26] Chaloupka J and Khaliullin G 2016 *Phys. Rev. B* **94** 064435
[27] Winter S M, Li Y, Jeschke H O, and Valentí R 2016 *Phys. Rev. B* **93** 214431
[28] Rousochatzakis I, Reuther J, Thomale R, Rachel S, and Perkins N B 2015 *Phys. Rev. X* **5** 041035
[29] Yadav R, Bogdanov N A, Katukuri V M, Nishimoto S, van den Brink J, and Hozoi L 2016 *Sci. Rep.* **6** 37925
[30] Hickey C and Trebst S 2019 *Nat. Commun.* **10** 530
[31] Cao H B, Banerjee A, Yan J Q, Bridges C A, Lumsden M D, Mandrus D G, Tennant D A, Chakoumakos B C, and Nagler S E 2016 *Phys. Rev. B* **93** 134423
[32] Liu X, Berlijn T, Yin W G, Ku W, Tsvelik A, Kim Y J, Gretarsson H, Singh Y, Gegenwart P, and Hill J P 2011 *Phys. Rev. B* **83** 220403
[33] Ye F, Chi S, Cao H, Chakoumakos B C, Fernandez-Baca J A, Custelcean R, Qi T F, Korneta O B, and Cao G 2012 *Phys. Rev. B* **85** 180403
[34] Songvilay M, Robert J, Petit S, Rodriguez-Rivera J A, Ratcliff W D, Damay F, Balédent V, Jiménez-Ruiz M, Lejay P, Pachoud E, Hadj-Azzem A, Simonet V, and Stock C 2020 *Phys. Rev. B* **102** 224429
[35] Samarakoon A M, Chen Q, Zhou H, and Garlea V O 2021 *Phys. Rev. B* **104** 184415
[36] Chen W, Li X, Hu Z, Hu Z, Yue L, Sutarto R, He F, Iida K, Kamazawa K, Yu W, Lin X, and Li Y 2021 *Phys. Rev. B* **103** L180404
[37] Lee C H, Lee S, Choi Y S, Jang Z H, Kalaivanan R, Sankar R, and Choi K Y 2021 *Phys. Rev. B* **103** 214447
[38] Krüger W G F, Chen W, Jin X, Li Y, and Janssen L 2023 *Phys. Rev. Lett.* **131** 146702
[39] Yao W, Zhao Y, Qiu Y, Balz C, Stewart J R, Lynn J W, and Li Y 2023 *Phys. Rev. Res.* **5** L022045
[40] Gu Y, Li X, Chen Y, Iida K, Nakao A, Munakata K, Garlea V O, Li Y, Deng G, Zaliznyak I A, Tranquada J M, and Li Y 2024 *Phys. Rev. B* **109** L060410
[41] Hu Z, Chen Y, Cui Y, Li S, Li C, Xu X, Chen Y, Li X, Gu Y, Yu R, Zhou R, Li Y, and Yu W 2024 *Phys. Rev. B* **109** 054411
[42] Garlea V O and Sarkis C L 2024 arXiv:2410.11083 [cond-mat.str-el]
[43] Singh Y and Gegenwart P 2010 *Phys. Rev. B* **82** 064412
[44] Choi S K, Coldea R, Kolmogorov A N, Lancaster T, Mazin I I, Blundell S J, Radaelli P G, Singh Y, Gegenwart P, Choi K R, Cheong S W, Baker P J, Stock C, and Taylor J 2012 *Phys. Rev. Lett.* **108** 127204
[45] Johnson R D, Williams S C, Haghighirad A A, Singleton J, Zapf V, Manuel P, Mazin I I, Li Y, Jeschke H O, Valentí R, and Coldea R 2015 *Phys. Rev. B* **92** 235119
[46] Mu S, Dixit K D, Wang X, Abernathy D L, Cao H, Nagler S E, Yan J, Lampen-Kelley P, Mandrus D, Polanco C A, Liang L, Halász G B, Cheng Y, Banerjee A, and Berlijn T 2022 *Phys. Rev. Res.* **4** 013067
[47] Zhang H, McGuire M A, May A F, Chao H Y, Zheng Q, Chi M, Sales B C, Mandrus D G, Nagler S E, Miao H, Ye F, and Yan J 2024 *Phys. Rev. Mater.* **8** 014402
[48] Park S Y, Do S H, Choi K Y, Jang D, Jang T H, Scheffer J, Wu C M, Gardner J S, Park J M S, Park J H, and Ji S 2024 *J. Phys.: Condens. Matter* **36** 215803
[49] Kim S, Horsley E, Nelson C, Ruff J, and Kim Y J 2024 arXiv:2403.04176 [cond-mat.strel]
[50] Regnault L P, Burlet P, and Rossat-Mignod J 1977 *Physica B+C* **86** 660
[51] Halloran T, Desrochers F, Zhang E Z, Chen T, Chern L E, Xu Z, Winn B, Graves-Brook M, Stone M B, Kolesnikov A I, Qiu Y, Zhong R, Cava R, Kim Y B, and Broholm C 2023 *Proc. Natl. Acad. Sci. U.S.A.* **120** e2215509119
[52] Dufault E, Bahrami F, Streeter A, Yao X, Gonzalez E, Zhang Q, and Tafti F 2023 *Phys. Rev. B* **108** 064405
[53] Zhong R, Gao T, Ong N P, and Cava R J 2020 *Sci. Adv.* **6** eaay6953
[54] Viciu L, Huang Q, Morosan E, Zandbergen H W, Greenbaum N I, McQueen T, and Cava R J 2007 *J. Solid State Chem.* **180** 1060
[55] Regnault L P, Boullier C, and Lorenzo J E 2018 *Heliyon* **4** e00507
[56] Li X, Gu Y, Chen Y, Garlea V O, Iida K, Kamazawa K, Li Y, Deng G, Xiao Q, Zheng X, Ye Z, Peng Y, Zaliznyak I A, Tranquada J M, and Li Y 2022 *Phys. Rev. X* **12** 041024
[57] Mazin I I, Jeschke H O, Foyevtsova K, Valentí R, and Khomskii D I 2012 *Phys. Rev. Lett.* **109** 197201
[58] Foyevtsova K, Jeschke H O, Mazin I I, Khomskii D I, and Valentí R 2013 *Phys. Rev. B* **88** 035107
[59] Streltsov S, Mazin I I, and Foyevtsova K 2015 *Phys. Rev. B* **92** 134408
[60] Gretarsson H, Clancy J P, Liu X, Hill J P, Bozin E, Singh Y, Manni S, Gegenwart P, Kim J, Said A H, Casa D, Gog T, Upton M H, Kim H S, Yu J, Katukuri V M, Hozoi L, van den Brink J, and Kim Y J 2013 *Phys. Rev. Lett.* **110** 076402
[61] Mazin I I, Manni S, Foyevtsova K, Jeschke H O, Gegenwart P, and Valentí R 2013 *Phys. Rev. B* **88** 035115
[62] Kim B H, Shirakawa T, and Yunoki S 2016 *Phys. Rev. Lett.* **117** 187201
[63] Kim B H, Khaliullin G, and Min B I 2014 *Phys. Rev. B* **89** 081109
[64] Igarashi J I and Nagao T 2015 *J. Phys.: Condens. Matter* **28** 026006
[65] Suzuki H, Gretarsson H, Ishikawa H, Ueda K, Yang Z, Liu H, Kim H, Kukusta D, Yaresko A, Minola M *et al.* 2019 *Nature materials* **18** 563
[66] Lebert B W, Kim S, Kim B H, Chun S H, Casa D, Choi J, Agrestini S, Zhou K, Garcia-Fernandez M, and Kim Y J 2023 *Phys. Rev. B* **108** 155122
[67] Diop S S, Jackeli G, and Savary L 2022 *Phys. Rev. B* **105** 144431
[68] Henley C L 1989 *Phys. Rev. Lett.* **62** 2056

[69] Sheng Q and Henley C L 1992 *J. Phys.: Condens. Matter* **4** 2937
[70] Schick R, Ziman T, and Zhitomirsky M E 2020 *Phys. Rev. B* **102** 220405
[71] Liu C, Yu R, and Wang X 2016 *Phys. Rev. B* **94** 174424
[72] Seabra L, Sindzingre P, Momoi T, and Shannon N 2016 *Phys. Rev. B* **93** 085132
[73] Mühlbauer S, Binz B, Jonietz F, Pfleiderer C, Rosch A, Neubauer A, Georgii R, and Böni P 2009 *Science* **323** 915
[74] Bogdanov A and Hubert A 1994 *J. Magn. Magn. Mater.* **138** 255
[75] Kanazawa N, Onose Y, Arima T, Okuyama D, Ohoyama K, Wakimoto S, Kakurai K, Ishiwata S, and Tokura Y 2011 *Phys. Rev. Lett.* **106** 156603
[76] Nakatsuji S, Kiyohara N, and Higo T 2015 *Nature* **527** 212
[77] Takagi R, White J S, Hayami S, Arita R, Honecker D, Rønnow H M, Tokura Y, and Seki S 2018 *Sci. Adv.* **4** eaau3402
[78] Rößler U K, Bogdanov A N, and Pfleiderer C 2006 *Nature* **442** 797
[79] Ishiwata S, Nakajima T, Kim J H, Inosov D S, Kanazawa N, White J S, Gavilano J L, Georgii R, Seemann K M, Brandl G, Manuel P, Khalyavin D D, Seki S, Tokunaga Y, Kinoshita M, Long Y W, Kaneko Y, Taguchi Y, Arima T, Keimer B, and Tokura Y 2020 *Phys. Rev. B* **101** 134406
[80] Paddison J A M, Zhang H, Yan J, Cliffe M J, McGuire M A, Do S H, Gao S, Stone M B, Dahlbom D, Barros K *et al.* 2024 *npj Quantum Materials* **9** 48
[81] Allred J M, Taddei K M, Bugaris D E, Krogstad M J, Lapidus S H, Chung D Y, Claus H, Kanatzidis M G, Brown D E, Kang J, Fernandes R M, Eremin I, Rosenkranz S, Chmaissem O, and Osborn R 2016 *Nat. Phys.* **12** 493
[82] Allred J M, Avci S, Chung D Y, Claus H, Khalyavin D D, Manuel P, Taddei K M, Kanatzidis M G, Rosenkranz S, Osborn R, and Chmaissem O 2015 *Phys. Rev. B* **92** 094515
[83] Taddei K M, Allred J M, Bugaris D E, Lapidus S, Krogstad M J, Stadel R, Claus H, Chung D Y, Kanatzidis M G, Rosenkranz S, Osborn R, and Chmaissem O 2016 *Phys. Rev. B* **93** 134510
[84] Kawarazaki S, Sato M, Miyako Y, Chigusa N, Watanabe K, Metoki N, Koike Y, and Nishi M 2000 *Phys. Rev. B* **61** 4167
[85] Khanh N D, Nakajima T, Hayami S, Gao S, Yamasaki Y, Sagayama H, Nakao H, Takagi R, Motome Y, Tokura Y *et al.* 2022 *Adv. Sci.* **9** 2105452
[86] Wood G D A, Khalyavin D D, Mayoh D A, Bouaziz J, Hall A E, Holt S J R, Orlandi F, Manuel P, Blügel S, Staunton J B, Petrenko O A, Lees M R, and Balakrishnan G 2023 *Phys. Rev. B* **107** L180402
[87] Saito H, Kon F, Hidaka H, Amitsuka H, Kwanghee C, Hagihala M, Kamiyama T, Itoh S, and Nakajima T 2023 *Phys. Rev. B* **108** 094440
[88] Okubo T, Nguyen T H, and Kawamura H 2011 *Phys. Rev. B* **84** 144432
[89] Okubo T, Chung S, and Kawamura H 2012 *Phys. Rev. Lett.* **108** 017206
[90] Kamiya Y and Batista C D 2014 *Phys. Rev. X* **4** 011023
[91] Hayami S, Lin S Z, and Batista C D 2016 *Phys. Rev. B* **93** 184413
[92] Hayami S and Motome Y 2019 *Phys. Rev. B* **99** 094420
[93] Hayami S and Motome Y 2021 *Phys. Rev. B* **103** 054422
[94] Yambe R and Hayami S 2023 *Phys. Rev. B* **107** 174408
[95] Yu R, Yi M, Frandsen B A, Birgeneau R J, and Si Q 2017 arXiv:1706.07087 [cond-mat.supr-con]
[96] Hayami S, Ozawa R, and Motome Y 2017 *Phys. Rev. B* **95** 224424
[97] Fang Y W, Yang R, and Chen H 2019 *J. Phys.: Condens. Matter* **31** 445803
[98] Paul S, Haldar S, von Malottki S, and Heinze S 2020 *Nat. Commun.* **11** 4756
[99] Kato Y and Motome Y 2022 *Phys. Rev. B* **105** 174413
[100] Hayami S 2023 *Phys. Rev. B* **108** 094415
[101] Hayami S and Yambe R 2024 *Materials Today Quantum* **3** 100010
[102] Pohle R, Shannon N, and Motome Y 2023 *Phys. Rev. B* **107** L140403
[103] Martin I and Batista C D 2008 *Phys. Rev. Lett.* **101** 156402
[104] Kato Y, Martin I, and Batista C D 2010 *Phys. Rev. Lett.* **105** 266405
[105] Ozawa R, Hayami S, and Motome Y 2017 *Phys. Rev. Lett.* **118** 147205
[106] Yang H Y, Albuquerque A F, Capponi S, Läuchli A M, and Schmidt K P 2012 *New J. Phys.* **14** 115027
[107] Swain N, Tiwari R, and Majumdar P 2016 *Phys. Rev. B* **94** 155119
[108] Kawarazaki S, Fujita K, Yasuda K, Sasaki Y, Mizusaki T, and Hirai A 1988 *Phys. Rev. Lett.* **61** 471
[109] Forgan E M, Rainford B D, Lee S L, Abell J S, and Bi Y 1990 *J. Phys.: Condens. Matter* **2** 10211
[110] Normile P S, Stirling W G, Mannix D, Lander G H, Wastin F, Rebizant J, Boudarot F, Burlet P, Lebech B, and Coburn S 2002 *Phys. Rev. B* **66** 014405
[111] Forgan E M, Gibbons E P, McEwen K A, and Fort D 1989 *Phys. Rev. Lett.* **62** 470
[112] Yue L, Ren X, Han T, Guo J, Wu Z, Zhang Y, and Li Y 2017 *Phys. Rev. B* **96** 180505
[113] Jensen J and Bak P 1981 *Phys. Rev. B* **23** 6180
[114] Burlet P, Ressouche E, Malaman B, Welter R, Sanchez J P, and Vulliet P 1997 *Phys. Rev. B* **56** 14013
[115] Park P, Cho W, Kim C, An Y, Kang Y G, Avdeev M, Sibille R, Iida K, Kajimoto R, Lee K H *et al.* 2023 *Nat. Commun.* **14** 8346
[116] Park P, Cho W, Kim C, An Y, Iida K, Kajimoto R, Matin S, Zhang S S, Batista C D, and Park J G 2024 arXiv:2410.02180 [cond-mat.str-el]
[117] Dong Y, Zhang B, Cao Y, Guo H, Ren W, Zhang A, Li Z, Wei Z, Liu H, Tang L, Pang H, Li F, and Li Z 2024 *Phys. Rev. B* **109** 094401
[118] Gastiasoro M N, Eremin I, Fernandes R M, and Andersen B M 2017 *Nat. Commun.* **8** 14317
[119] Spethmann J, Meyer S, von Bergmann K, Wiesendanger R, Heinze S, and Kubetzka A 2020 *Phys. Rev. Lett.* **124** 227203
[120] Tokunaga Y, Homma Y, Kambe S, Aoki D, Sakai H, Yamamoto E, Nakamura A, Shiokawa Y, Walstedt R E, and Yasuoka H 2005 *Phys. Rev. Lett.* **94** 137209
[121] Jin X, Geng M, Orlandi F, Khalyavin D, Manuel P, Liu Y, and Li Y 2025 arXiv:2501.07843 [cond-mat.str-el]
[122] Wang J and Liu Z X 2023 *Phys. Rev. B* **108** 014437
[123] Shimokawa T, Okubo T, and Kawamura H 2019 *Phys. Rev. B* **100** 224404
[124] Yao W and Li Y 2020 *Phys. Rev. B* **101** 085120
[125] Miao P, Jin X, Yao W, Chen Y, Koda A, Tan Z, Xie W, Ji W, Kamiyama T, and Li Y 2024 *Phys. Rev. B* **109** 134431
[126] Yao W, Iida K, Kamazawa K, and Li Y 2022 *Phys. Rev. Lett.* **129** 147202
[127] Lin G, Jeong J, Kim C, Wang Y, Huang Q, Masuda T, Asai S, Itoh S, Günther G, Russina M *et al.* 2021 *Nat. Commun.* **12** 5559
[128] Kim C, Jeong J, Lin G, Park P, Masuda T, Asai S, Itoh S, Kim H S, Zhou H, Ma J, and Park J G 2021 *J. Phys.: Condens. Matter* **34** 045802
[129] Singh Y, Manni S, Reuther J, Berlijn T, Thomale R, Ku W, Trebst S, and Gegenwart P 2012 *Phys. Rev. Lett.* **108** 127203

[130] Janssen L, Andrade E C, and Vojta M 2016 *Phys. Rev. Lett.* **117** 277202

[131] Chern G W, Sizyuk Y, Price C, and Perkins N B 2017 *Phys. Rev. B* **95** 144427

[132] Winter S M 2022 *J. Phys. Mater.* **5** 045003

[133] Wellm C, Roscher W, Zeisner J, Alfonsov A, Zhong R, Cava R J, Savoyant A, Hayn R, van den Brink J, Büchner B, Janson O, and Kataev V 2021 *Phys. Rev. B* **104** L100420

[134] Nair H S, Brown J M, Coldren E, Hester G, Gelfand M P, Podlesnyak A, Huang Q, and Ross K A 2018 *Phys. Rev. B* **97** 134409

[135] Maksimov P A, Ushakov A V, Pchelkina Z V, Li Y, Winter S M, and Streltsov S V 2022 *Phys. Rev. B* **106** 165131

[136] Francini N and Janssen L 2024 *Phys. Rev. B* **109** 075104

[137] Francini N and Janssen L 2024 *Phys. Rev. B* **110** 235118

[138] Merino J and Ralko A 2018 *Phys. Rev. B* **97** 205112

[139] Zhu Z and White S R 2014 *Mod. Phys. Lett. B* **28** 1430016

[140] Bishop R F, Li P H Y, Farnell D J J, and Campbell C E 2012 *J. Phys.: Condens. Matter* **24** 236002

[141] Bose A, Routh M, Voleti S, Saha S K, Kumar M, Saha-Dasgupta T, and Paramekanti A 2023 *Phys. Rev. B* **108** 174422

[142] Shi L Y, Wang X M, Zhong R D, Wang Z X, Hu T C, Zhang S J, Liu Q M, Dong T, Wang F, and Wang N L 2021 *Phys. Rev. B* **104** 144408

[143] Zhang X S, Xu Y Y, Halloran T, Zhong R D, Broholm C, Cava R J, Drichko N, and Armitage N P 2023 *Nat. Mater.* **22** 58

[144] Jiao J L, Li X Y, Lin G T, Shu M, Xu W, Zaharko O, Shiroka T, Hong T, Kolesnikov A I, Deng G *et al.* 2024 *Commun. Mater.* **5** 159

[145] Lefrançois É, Grissonnanche G, Baglo J, Lampen-Kelley P, Yan J Q, Balz C, Mandrus D, Nagler S E, Kim S, Kim Y J, Doiron-Leyraud N, and Taillefer L 2022 *Phys. Rev. X* **12** 021025

[146] Lefrançois É, Baglo J, Barthélemy Q, Kim S, Kim Y J, and Taillefer L 2023 *Phys. Rev. B* **107** 064408

[147] Sears J, Shen Y, Krogstad M J, Miao H, Yan J, Kim S, He W, Bozin E S, Robinson I K, Osborn R, Rosenkranz S, Kim Y J, and Dean M P M 2023 *Phys. Rev. B* **108** 144419

[148] Hong X, Gillig M, Yao W, Janssen L, Kocsis V, Gass S, Li Y, Wolter A U, Büchner B, and Hess C 2024 *npj Quantum Materials* **9** 18

[149] Takeda H, Mai J, Akazawa M, Tamura K, Yan J, Moovendaran K, Raju K, Sankar R, Choi K Y, and Yamashita M 2022 *Phys. Rev. Res.* **4** L042035